# Experimental Studies of the Quasi-binary System Na<sub>2</sub>SO<sub>4</sub> – NiSO<sub>4</sub> by Differential Thermal Analysis, Calorimetry and X-Ray Diffraction

D. Kobertz, D. Sergeev and M. Müller

Forschungszentrum Jülich, IEK-2, D-52425 Jülich, Germany, email: d.kobertz@outlook.de

Keywords: corrosion, thermodynamic, Nickel sulfate, Sodium sulfate, Phase diagram

#### **Abstract**

This work is dedicated to experimental studies of the quasi-binary sub-system  $Na_2SO_4$  -  $NiSO_4$  with Differential Thermal Analysis (DTA) with simultaneous Thermal Gravimetry (TG), Differential Scanning Calorimetry (DSC), and X-ray Diffraction (XRD) to obtain the transition temperatures, the phase compositions, and thermodynamic data of  $Na_2Ni(SO_4)_2$ , ( $Fp: 982 \pm 3$  K,  $\Delta H_{fus} = 59 \pm 3$  kJ mol<sup>-1</sup>), compound in this sulfate system. A compound  $Na_6Ni(SO_4)_4$ ) with the decomposition temperature  $682 \pm 3$  K was confirmed. The lack in the data of the NiSO<sub>4</sub>-rich region was clarified. The entire composition range could be measured and the structure change at  $1243 \pm 3$  K ("dkostruct") that enables to describes corrosion processes on Ni- containing alloys in a sulphatic-rich environmental, as well as the melting point of NiSO<sub>4</sub> at  $1483 \pm 3$  K could be confirmed in this work. A new and complete phase diagram was determined.

#### Introduction

Hot corrosion on turbine blading is initiated by deposition or condensation of corrosive species like alkali sulfates and dependent on concentrations of alkalis in the hot flue gas.

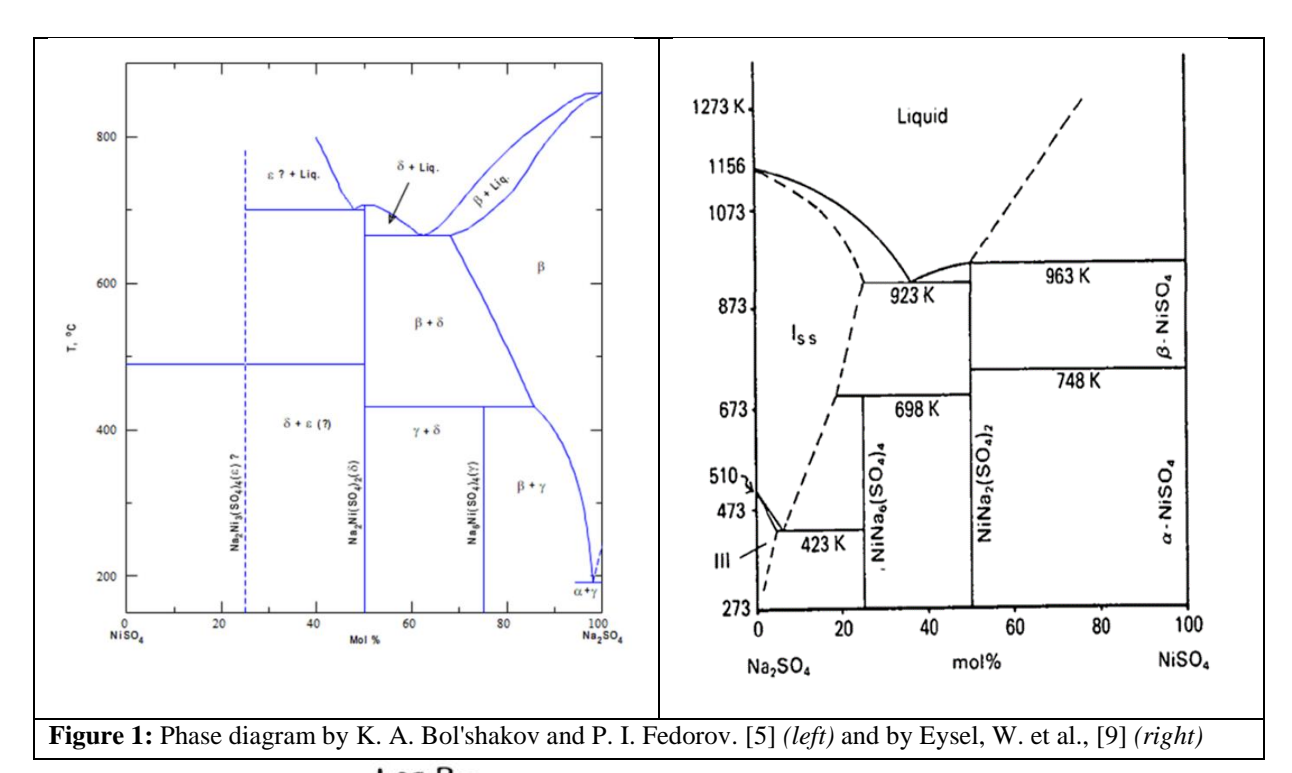
Type I hot corrosion is triggered by the formation of liquid Na<sub>2</sub>SO<sub>4</sub> above its melting point (884 °C) (Pettit [1]).

Type II hot corrosion is caused by the formation of an eutectic melt of NiSO<sub>4</sub> and Na<sub>2</sub>SO<sub>4</sub> above 671 °C. NiSO<sub>4</sub> itself is formed by the reaction of the oxide scale of Ni based alloys in blading with SO<sub>3</sub> in dependence of the SO<sub>3</sub> partial pressure in the hot flue gas (Wang et al. [2]).

The motivation of our studies is to understand the aforementioned alkali sulfate related processes under applied conditions and accrued phases. This work includes the experimental studies of the complete quasi-binary sub-systems Na<sub>2</sub>SO<sub>4</sub> - NiSO<sub>4</sub>. In the literature [3-17] are variant and uncompleted contradictory results and interpretations regarding phase diagrams and pure NiSO<sub>4</sub> and always with a gap in the NiSO<sub>4</sub> - rich part. Differential Thermal Analysis (DTA) with simultaneous Thermal Gravimetry (TG), as well as X-ray Diffraction (XRD) measurements were done both to achieve the transition temperatures and the phase compositions in this sulfate system. A new phase diagram was determined.

Two phase diagrams in literature of Bol'shakov et al. [5] (figure 1, left) and Eysel, W. et al. [9] (figure 1, right), both are experimental ones, present phase lines in their phase diagram, that are different. Common in both is the existence of the two compounds 1:1 and 3:1. Cot [7] describes the existence of  $Na_2Ni(SO_4)_2$  as an anhydride and hydrate using thermal analysis and XRD.

Stable phases in the System Na-Ni-S-O at 900 °C (figure 2) depending on the partial pressure of O<sub>2</sub> and the activity of Na<sub>2</sub>O by Rapp, R. A. [10] show the stability regions of NiSO<sub>4</sub> at conditions driving high temperature turbines. Similar situation is given in the Ni-S-O<sub>2</sub> system depending on the partial pressures of S and O<sub>2</sub> by Roslik, A.K., V.N. Konev, and A.M. Maltsev, [12] and by Shariat, M. H.; Behgozin, S. A. [18].



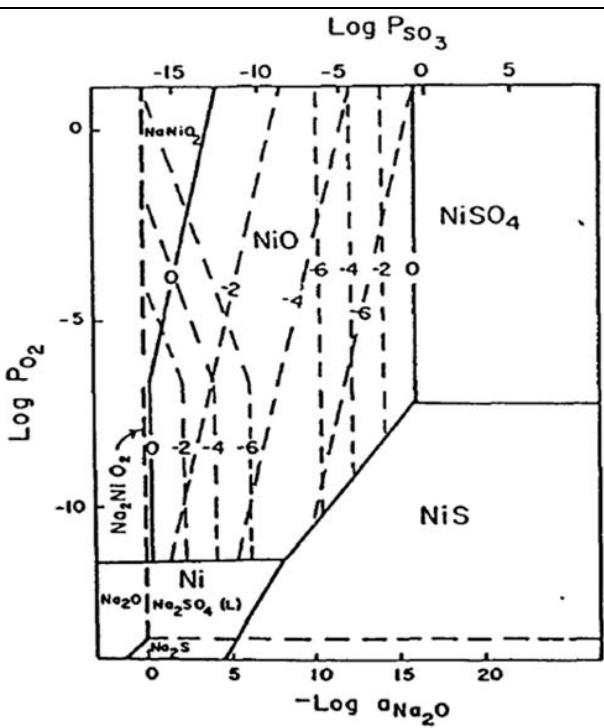


**Figure 2:** Stable phases in the System Na-Ni-S-O at 900 °C depending on the partial pressure of  $O_2$  and the activity of  $Na_2O$  by Rapp, R. A. [10]

## **Experimental**

## Differential Thermal Analysis (DTA) with simultaneous Thermal Gravimetry (TG))

Anhydrous pure NiSO<sub>4</sub> (nominal purity 99.99 mass %, and pure Na<sub>2</sub>SO<sub>4</sub> (nominal purity 99.99 mass %, (both, SIGMA-ALDRICH, Saint Louis, USA) and mixtures of them (x) Na<sub>2</sub>SO<sub>4</sub> – (1-x) NiSO<sub>4</sub> (x=0 - 100) covering the complete range of the quasi-binary phase diagram were measured in a first step in open Al<sub>2</sub>O<sub>3</sub>, quartz, and platinum crucibles. Sulfate systems are sensitive in stability concerning the variation of the equilibrium state. Since the pressure equilibrium constant is depending on the partial pressures of SO<sub>2</sub> and O<sub>2</sub>, a change in partial pressures can force a decomposition process. Later, to achieve equilibrium state, mixtures were studied in sealed quartz (figure 3) and platinum crucible. The advantage of quartz container was the evacuation of the system down to 100 Pa via a valve adapter. Traces of possible moisture were removed by heating the sample up to 500 °C before sealing the crucible. In contrast to this platinum crucible show more distinct tendency in DTA signal.

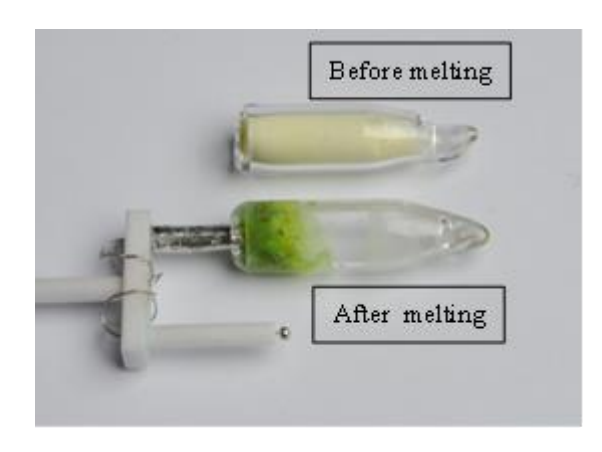


**Figure 3:** Sealed quartz crucible ([19]) here instancing filled with pure NiSO<sub>4</sub> before and after DTA experiment.

The hygroscopic nature of Nickel sulfate [14] requires a process of preparation and handling in a glove-box under argon. For a sufficient sample to crucible mass rate, about 300 to 400 mg sample were prepared in the container. Studies by the high temperature Simultaneous Thermal Analyzer (STA 429, Netzsch,

Selb, Germany) method followed well defined temperature programs with a standard rate of 5 K/min. Different heating and cooling rates of both, 2 and 10 K/min supported the analysis of super-cooling behavior and scrutiny of DTA responds. Simultaneously, a balance recorded the mass and allowed to find out the beginning of possible weight loss due to decomposition concerning runs in open crucibles.

Transition temperatures were measured with a thermocouple type S (Pt/(Pt 10%Rh)). An easy way to calibrate the thermocouple is with certified reference samples and their transition temperatures. The calibration runs with SiO<sub>2</sub> (571 °C),  $K_2SO_4$  (582 °C),  $BaCO_3$  (808 °C),  $SrCO_3$  (928 °C), Ag (961 °C) and Au (1064 °C) under the same condition like the studies on NiSO<sub>4</sub> (Kobertz et al. [19]) yielded in an estimated accuracy of the observed thermal effects of  $\pm$  3 K.

The ambiance during the measurements in open cells was dynamic with 100 ml/min in both, argon, and dry air. In terms of contrastable results, the dynamic flow rate was the same also on studies with sealed crucible.

The characteristic inception temperatures of the DTA curves, representing phase transitions were evaluated by the determination of the intersection of the extrapolated baseline and the tangent at the point of greatest slope on the leading edge of the peak (onset determination). More about the experimental details see Kobertz et al. [19]

#### **Differential scanning calorimetry (DSC)**

Two differential scanning calorimeters were used for the determination of thermodynamic properties. The main parameters of these devices are given in Table 1.

**Table 1**. Parameters of the differential scanning calorimeters.

Instrument	DSC 404C_HighT	DSC 404C_LowT		
Company	Netzsch, Selb, Germany			
Temperature range	25 °C -1600 °C	-180 °C – 650 °C		
Thermocouple	Type S	Туре К		
Oven (heating element)	Pt-Rh	Ag		
Heating rate	15 K/min	20 K/min		
Atmosphere	He, 10 ml/min	He, 10 ml/min		
Sample weight	20-50 mg	20-50 mg		
Crucible	Pt	Pt		

The ratio method with sapphire as a reference was applied for determination of the heat capacity ( $C_p^{\circ}$ , J·mol<sup>-1</sup>·K<sup>-1</sup>) according to the following equation (1):

$$C_{p(s)}^{0} = \frac{m_r}{m_s} \cdot \frac{DSC_s - DSC_b}{DSC_r - DSC_b} \cdot C_{p(r)}^{0} \tag{1}$$

where m – mass of the substance (g), DSC – signal of thermopile ( $\mu V$ ), r – reference, s – sample, b - baseline. The reference was a sapphire slice of mass comparable to that of the sample mass. Baseline and reference measurements were performed for each measured sample separately.

Beside thermal analysis, a set of different compositions with four samples each and sealed in quartz and platinum crucible were heat treated over a period of three weeks. For the history to see the equilibration state, one sample of each composition was taken out of the furnace after every week, then quenched and analyzed immediately by XRD. It was found that the equilibrium state was already reached within the first week. The other sample stayed to continue the heat treatment and in the end the sample with the longest time was used to consider the final interpretation.

#### **Results and discussion**

#### NiSO<sub>4</sub> – rich part

A detailed description on pure NiSO<sub>4</sub> is given in Kobertz et al. [19]. In this work, the studies under free vaporization conditions in open crucibles confirmed the stoichiometric decomposition of NiSO<sub>4</sub>, but kinetically forced always at different temperatures, following the equation (2).

$$NiSO_4(s) \leftrightarrow NiO(s) + SO_2(g) + \frac{1}{2}O_2(g)$$
 (2)

The highest measured decomposition temperature was at 920  $^{\circ}$ C. Since the equilibrium constant of equation (1) depends on the partial pressures of  $SO_2$  and  $O_2$ , one can imagine that once the reaction has started, the loss of non-condensable gases and with it the change in the equilibrium constant (Equation 3), keeps the decomposition process running.

$$Kp = p\left(SO_2\right) \cdot \sqrt{p\left(O_2\right)} \tag{3}$$

Equilibrium measurements are only possible in a closed system. Sealed platinum tubes showed unanticipated weight loss at temperatures about 960  $^{\circ}$ C, although there was no leak seen after cooling down. The reason for the weight loss is a permeability of platinum for SO<sub>2</sub> and O<sub>2</sub> at high temperature beyond 960  $^{\circ}$ C.

Samples with more than 70 mol% of NiSO<sub>4</sub> had to be measured in quartz. We found out that sealed quartz crucible remained stable up to  $10^6$  Pa. This is in line with the work of Wöhler et al. [4] and Roslik et al. [12] where they describe the expectable total pressure over NiSO<sub>4</sub> at 1200 °C is less than  $5.2 ext{ } 10^5$  Pa.

The DTA respond of measurements in sealed quartz crucible from pure NiSO<sub>4</sub> to the composition 72 mol% NiSO<sub>4</sub> – 28 mol% Na<sub>2</sub>SO<sub>4</sub> showed three transition temperatures, two constant one at 970 °C and 690 °C and a variable one from highest temperature at 1192 °C to 960 °C. Between 72 and 50 mol% only two transitions were observed with a constant one at 680 °C and a variable one that ends at the constant one.

The transition change at 970 °C is related to the structure change ("dkostruct", Kobertz et al. [19]) of NiSO<sub>4</sub> and the one at constant temperature of 690 °C concerns the eutectic temperature.

DTA studies in sealed container have the advantage to repeat the measurement without losing the composition. Seeing the history of the sample reaching the final equilibrium state is important to qualify the result.

In figure 4 is the summary of DTA responds of two sample with the composition 29 mol%  $Na_2SO_4 - 71$  mol%  $NiSO_4$  each measured two times. During the first heating run the sample is not yet in equilibrium and shows two and even three different temperatures around 700 °C. In the cooling segment only one temperature of 680 °C is observed. No further transitions below this temperature down to room temperature were found in the  $NiSO_4$  rich part of the phase diagram.

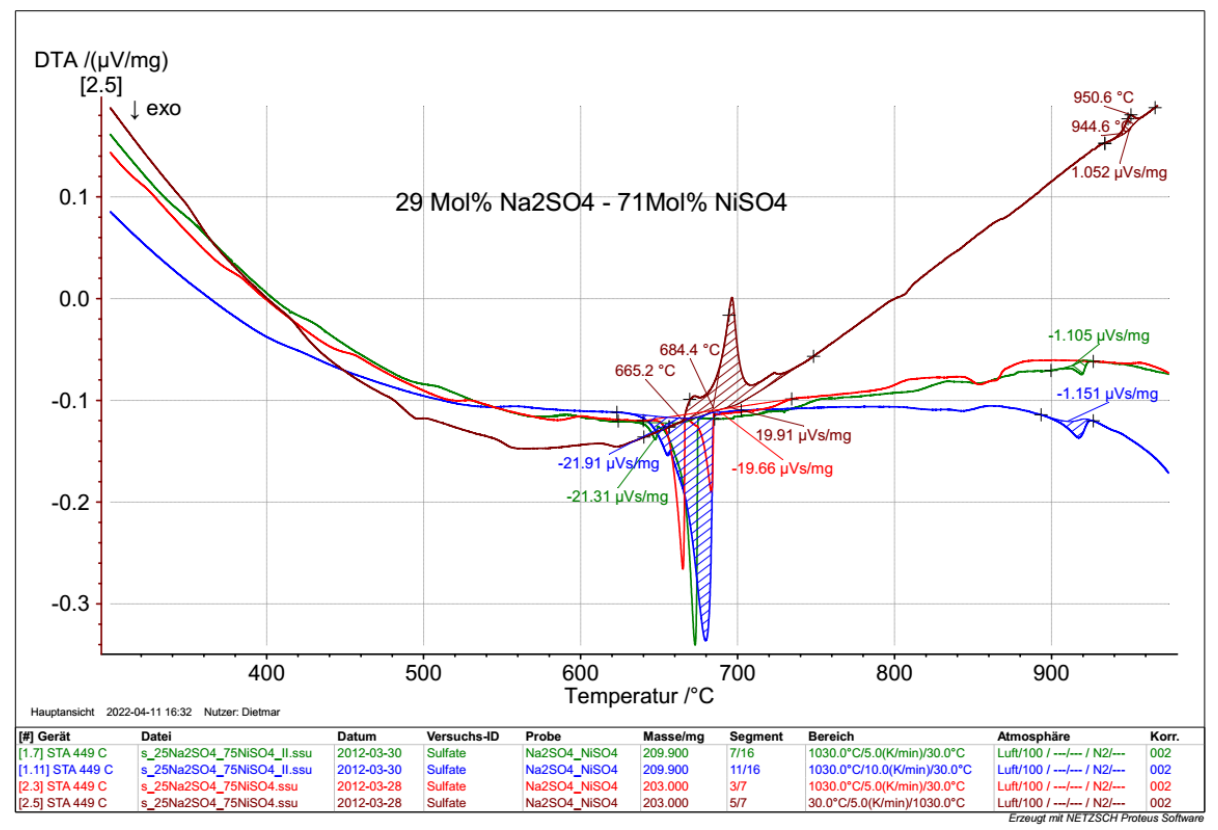


**Figure 4:** Repeated runs of two different 29 mol%  $Na_2SO_4 - 71$  mol%  $NiSO_4$  composition. For a better overview selected runs out of 16 (sample 1) and 7 (sample 2) are show. On heating and cooling at the beginning two peaks are observed around 680 °C (brown and red segment). On repeated measurements one peak is disappearing as seen in the green and blue lines. Finally, the equilibrium state of the sample is reached with single transition at 680 °C (eutectic line in figure 16). The upper peaks belong to the liquidus line and structure change. Temperatures in the figure are uncalibrated raw data.

From the XRD analysis it could be asserted that the NiSO<sub>4</sub>-rich solid-state region has only two coexisting phases of NiSO<sub>4</sub> and Na<sub>2</sub>Ni(SO<sub>4</sub>)<sub>2</sub> (figure 5)

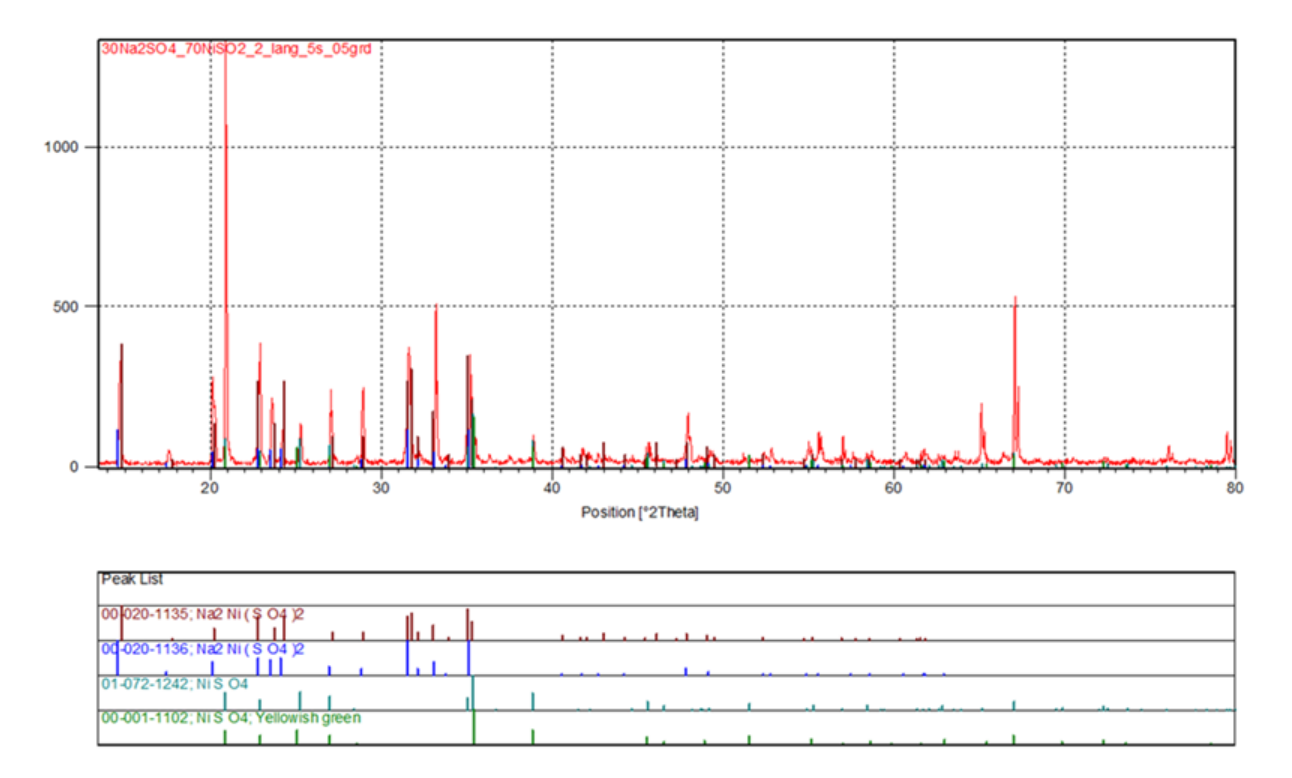


**Figure 5:** X-ray pattern of a quenched sample 30  $Na_2SO_4 - 70 NiSO_4$  (heat treatment at 600 °C, three weeks). Only two phases of  $NiSO_4$  and  $Na_2Ni(SO_4)_2$  could be observed.

The structure "dkostruct" at 970 °C expands in volume during cooling transition. This volume change results in a porous sulphate layer on a Ni-containing alloy. In a cycling process of temperature change on turbines around the structure transition it will be susceptible for further corrosion. The formation of the sulfate and reformation of decomposed NiO is fast at pressures >2 bar since the reaction in equation (1) is shifted to the left side. The fast reformation process was explained by Ingraham et al. [20]. Cycling of volume change in the layer opens induced micropores for the non-condensable partners in reaction (1) and that keeps the corrosion process running. This can explain the fast corrosion processes once the sulphate layer is produced.

The equimolar mixture (1:1) has a congruent melting temperature of 709 °C.

Concerning the results, the first half range of the phase diagram between pure NiSO<sub>4</sub> and the compound  $Na_2Ni(SO_4)_2$  (1:1) is a simple eutectic system with two NiSO<sub>4</sub> structures and an eutectic point at 44  $Na_2SO_4 - 56 NiSO_4$ .

#### Na<sub>2</sub>SO<sub>4</sub> rich part

platinum crucibles did not show permeability beyond 30 mol% Na<sub>2</sub>SO<sub>4</sub>. The studies in quartz and Pt showed comparable results.

DTA results supposed a compound beyond 50 mol% of Na<sub>2</sub>SO<sub>4</sub> with an unknow composition. A transition signal at constant temperature without endmembers concern a compound with a decomposition behavior.

In the range from  $Na_2Ni(SO_4)_2$  (1:1) up to 70%  $Na_2SO_4$  generally three transitions could be observed. Two at constant temperature of 409 °C respectively at 664 °C and one at a variable temperature between 730 °C and 664 °C.

#### Existence of a Na<sub>2</sub>SO<sub>4</sub> rich compound

The decomposition enthalpy as a function of the sample composition is dependent on the concentration of the sample in the heterogeneous phase region. The maximum is given at the pure compound and all other will be lower. With the Tammann-construction [21] it is possible to find the composition concentration. As a result, the 3:1 (Na<sub>6</sub>Ni(SO<sub>4</sub>)<sub>4</sub>) compound could be confirmed (figure 6).

# Tammankonstruction for Na<sub>6</sub>Ni(SO<sub>4</sub>)<sub>4</sub> (3:1)

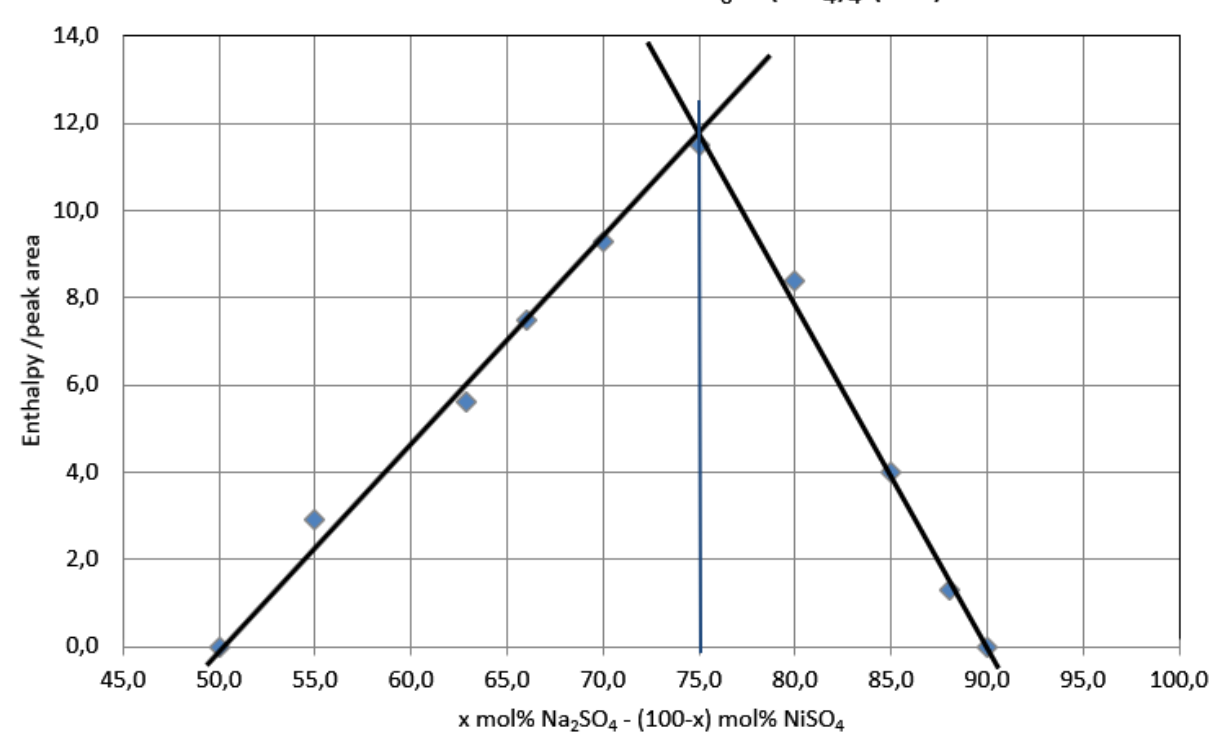


**Figure 6:** Tammann-construction [21] in the  $Na_2SO_4$ -rich region. The rhomb symbols represent the decomposition enthalpy as a function of the sample composition based on the peak area of the DTA signal. An enthalpy maximum is given at 75 mol%  $Na_2SO_4 - 25 NiSO_4$  (3:1)

To verify additionally the existence of the  $Na_6Ni(SO_4)_4$  and its decomposition at 409 °C, XRD pattern of heat-treated samples kept at 600 °C for three weeks with the composition of x  $Na_2SO_4$  – (100-x)  $NiSO_4$  (x/mol% = 70, 80 and 88) were drawn up.

Figures 7, 8, and 10 show XRD reflections of the quenched samples above the upper limit decomposition temperature of 409 °C. Samples with 70 and 80 mol%  $Na_2SO_4$  represent a two-phase region with structures of  $Na_2SO_4$  and  $Na_2Ni(SO_4)_2$  (1:1) and the sample with 88% is within a single phase, the solid solution of sodium sulfate.

Figures 9 and 11 show the results for the samples (x/mol% = 80, 88) after cooling down to room temperature. They show two phases with different structures, one with Na<sub>2</sub>SO<sub>4</sub> and another with a modified pattern related to Na<sub>6</sub>Mg(SO<sub>4</sub>)<sub>4</sub>. Since the sample 3:1 is not yet in the ICSD XRD data base [22] and Mg is not in the composition these reflections must be from Na<sub>6</sub>Ni(SO<sub>4</sub>)<sub>4</sub>.

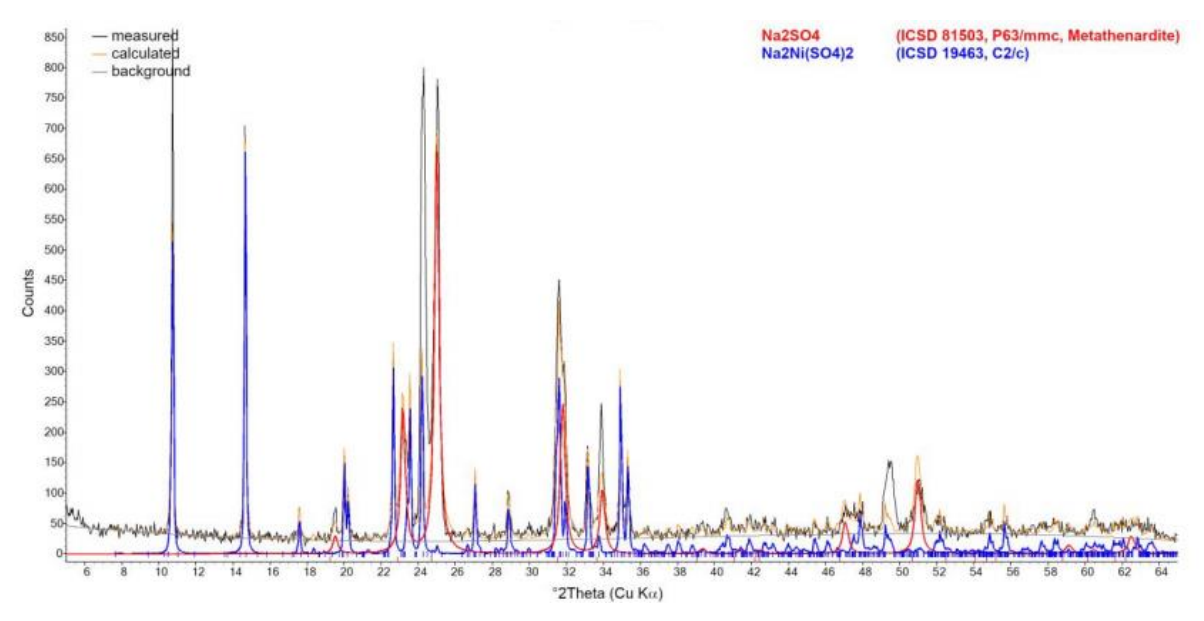


**Figure 7:** X-ray pattern of a quenched sample  $70 \text{ Na}_2\text{SO}_4 - 30 \text{ NiSO}_4$  (heat treatment at  $600 \,^{\circ}\text{C}$ , three weeks). Only two phases of  $\text{Na}_2\text{SO}_4$  and  $\text{Na}_2\text{Ni}(\text{SO}_4)_2$  could be observed above decomposition temperature of the compound 3:1.

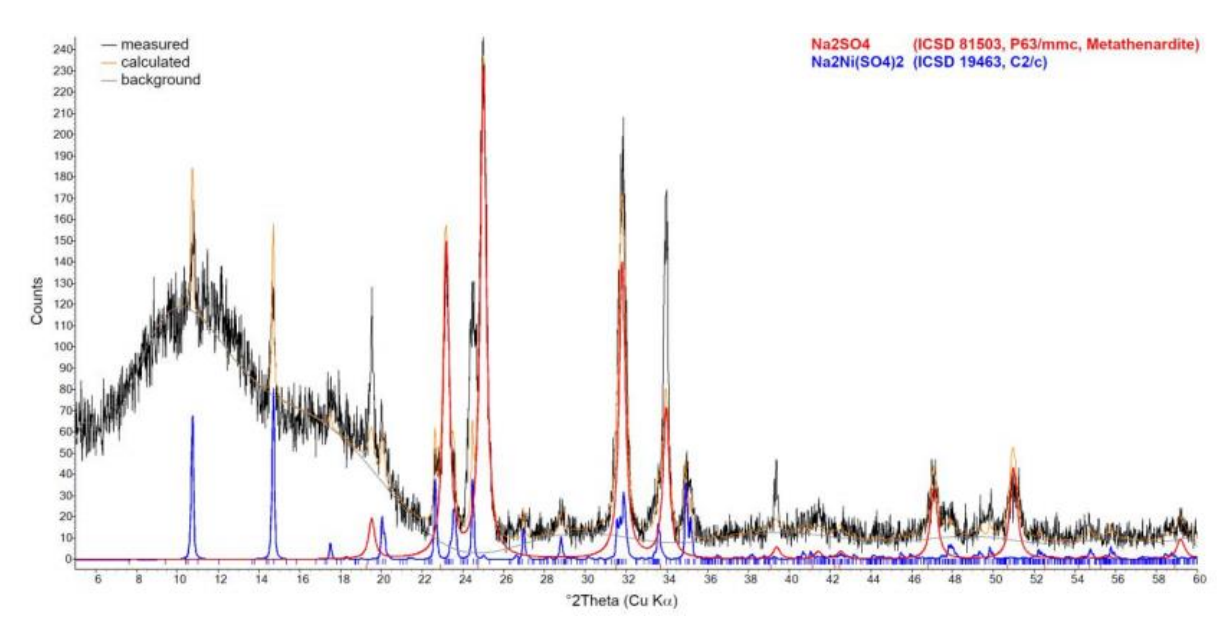


**Figure 8:** X-ray pattern of a quenched sample  $80 \text{ Na}_2\text{SO}_4 - 20 \text{ NiSO}_4$  (heat treatment at  $600 \,^{\circ}\text{C}$ , three weeks). Only two phases of  $\text{Na}_2\text{SO}_4$  and  $\text{Na}_2\text{Ni}(\text{SO}_4)_2$  could be observed above decomposition temperature of the compound 3:1

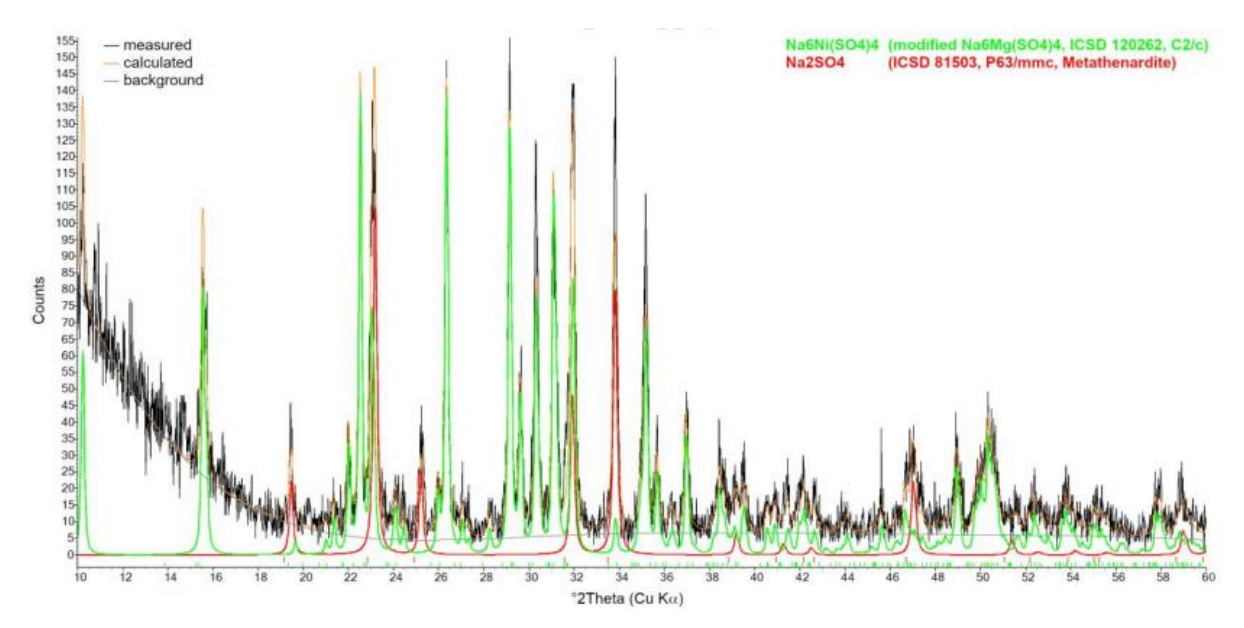


**Figure 9:** X-ray pattern of a sample  $80 \text{ Na}_2SO_4 - 20 \text{ NiSO}_4$  (heat treatment at  $600 \,^{\circ}\text{C}$ , three weeks) and cooled down below decomposition temperature of the compound 3:1. Only two phases of  $\text{Na}_2SO_4$  and  $\text{Na}_6\text{Ni}(SO_4)_4$  could be observed.

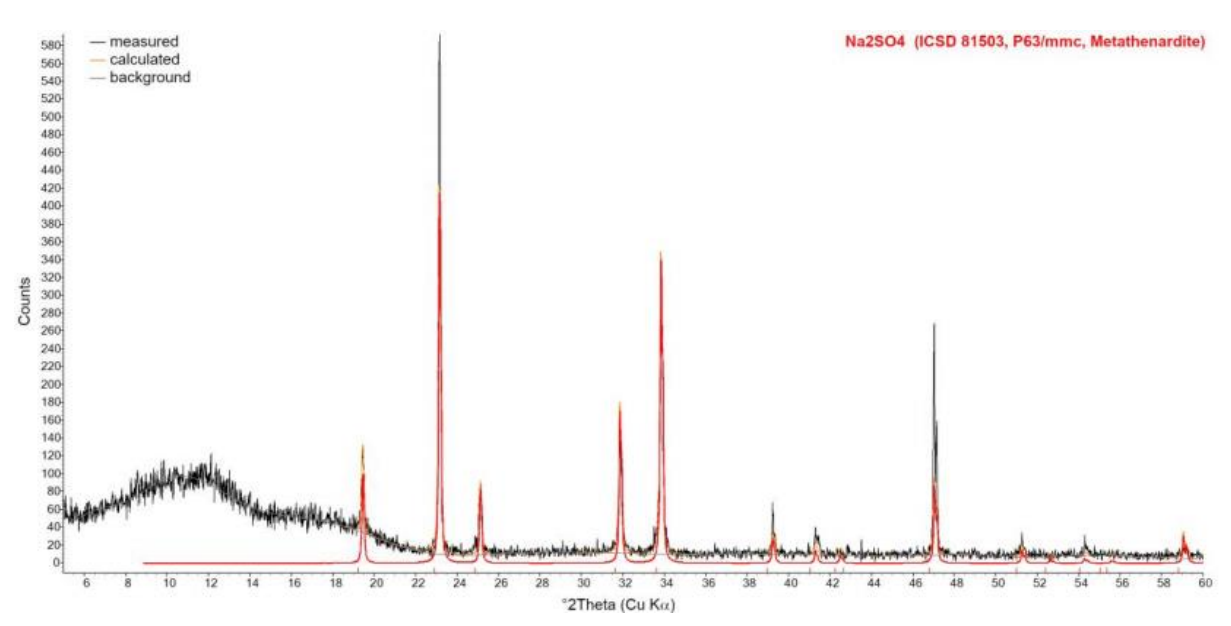
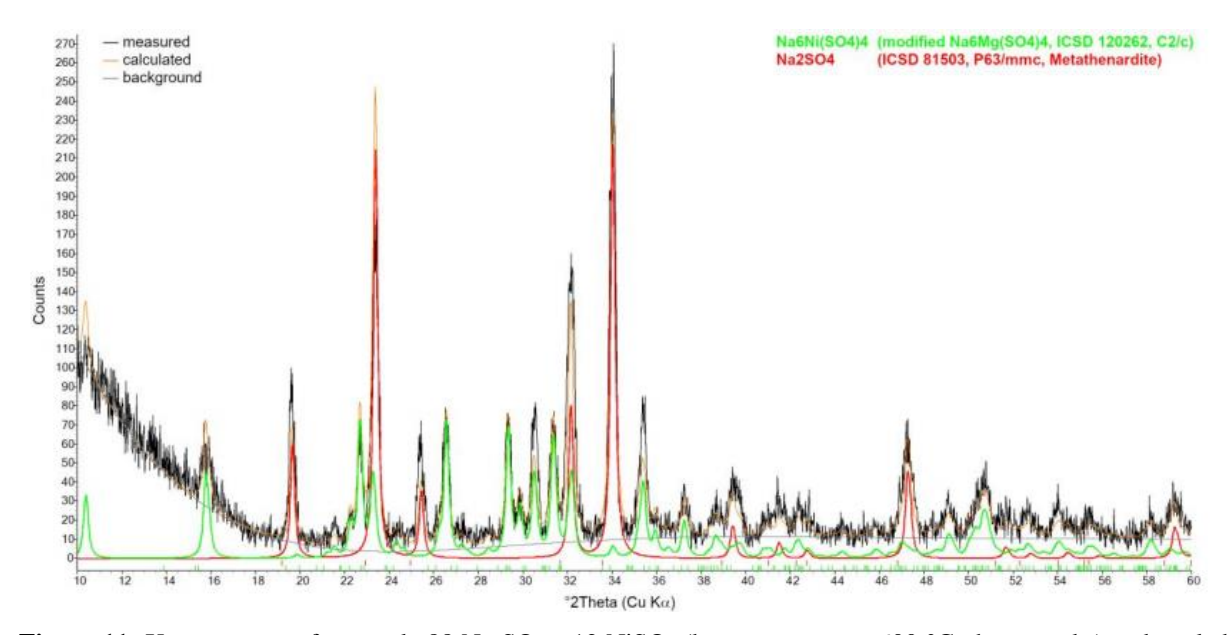


Figure 10: X-ray pattern of a quenched sample  $88 \text{ Na}_2\text{SO}_4 - 12 \text{ NiSO}_4$  (heat treatment at  $600 \,^{\circ}\text{C}$ , three weeks). Only one phase of Na<sub>2</sub>SO<sub>4</sub> could be observed above the decomposition temperature of the compound 3:1.



**Figure 11:** X-ray pattern of a sample 88  $Na_2SO_4 - 12$   $NiSO_4$  (heat treatment at 600 °C, three weeks) and cooled down below decomposition temperature of the compound 3:1. Only two phases of  $Na_2SO_4$  and  $Na_6Ni(SO_4)_4$  could be observed.

From the 3:1 compound to 100 mol% Na<sub>2</sub>SO<sub>4</sub> are two phases consisting of 3:1 and temperature dependent solid solutions with different modifications of Na<sub>2</sub>SO<sub>4</sub> ending at the solubility limit of the solid solution.

Below 200 °C two phases with 3:1 and pure  $Na_2SO_4$  were observe while beyond this temperature the phases 3:1 and the solid solution  $\alpha$ - $Na_2SO_4$  coexist up to a solubility limit from 100 to 87 mol%. Pure  $Na_2SO_4$  has two transitions in the DTA signal showing the two stable modifications at 210 (orthorhombic) and 250 °C (hexagonal) as described by Eysel et al. [9].

Four transitions were seen between 70 and 87 mol% Na<sub>2</sub>SO<sub>4</sub> with one constant at 409 °C and three variable one between 840 °C to 409 °C. They are related to the upper limit decomposition of the 3:1 compound, the solubility limit of the solid solution, and the solidus and liquidus lines.

Special interest was focussed on the 50 mol%  $Na_2SO_4 - 50$  mol%  $NiSO_4$  sample. Ten independent samples were prepared for DTA (seven) and DSC (three) measurements with multiple runs. Figure 12 shows a clearly represented compilation of selected runs after reaching the equilibrium state. Since any sample synthesis is never completely perfect, variation in the constitution is obvious. A systematic related deviation can be helpful to analyse the state around the system under consideration. One example of a deviation with a small surplus of  $Na_2SO_4$  in one of the prepared 1:1 sample described already the next phase region with the eutectic temperature at 664 °C and liquidus line (overlapping peak in expanded picture in figure 12).

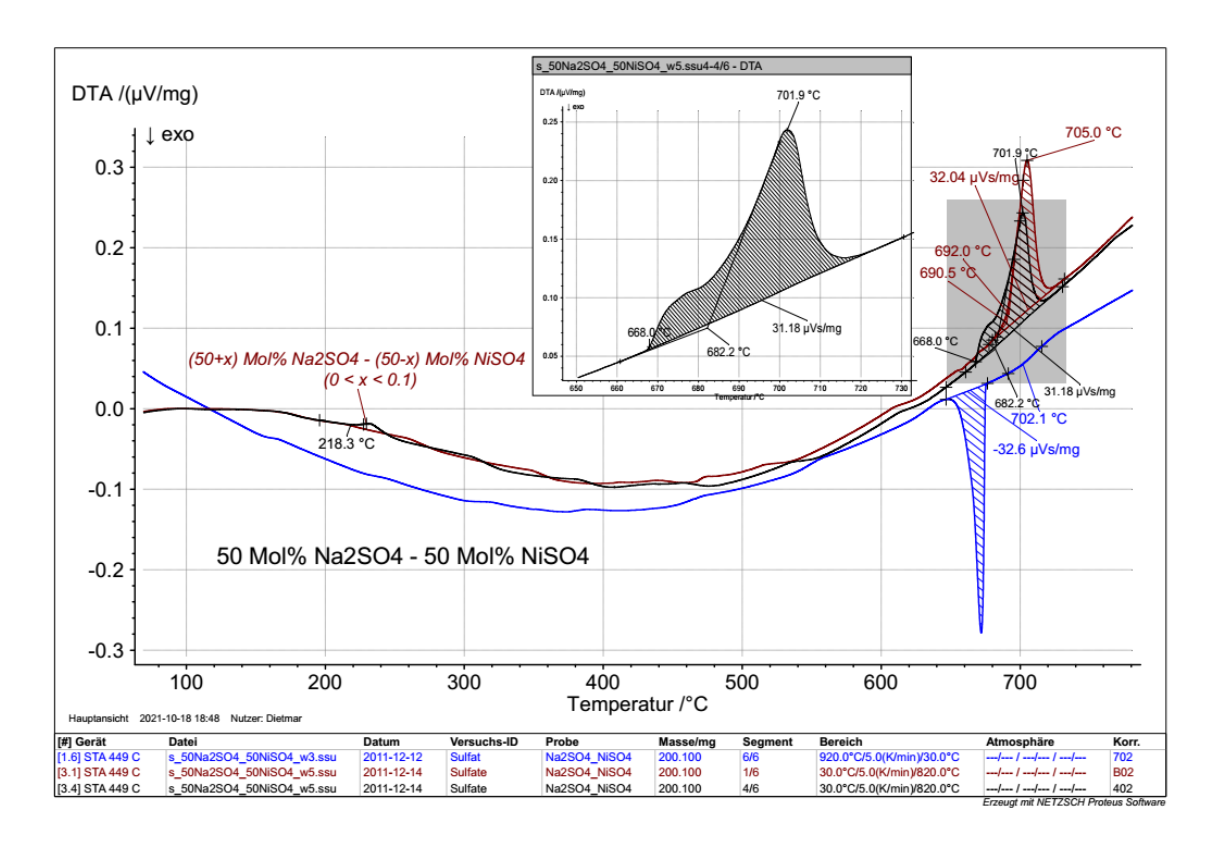


**Figure 12:** This figure shows a clearly repensented compilation of selected runs after reaching the equilibrium state. Also one example of a deviation with a small surplus of  $Na_2SO_4$  in the prepared 1:1 sample describes already the next phase region with the eutectic temperature at 664 °C and liquidus line in the expanded picture.

The history on the in-situ formation of 54 mol%  $Na_2SO_4 - 46$  mol%  $NiSO_4$  (figure 13) shows again the step-wise stages to reach the equilibrium state. Not until this state is reached the results are useless, and it should be pointed out that the first measurement must be repeated to find out consistent transition temperatures. The temperatures concern with the decomposition of the 3:1 compound (409 °C) and the eutectic (664 °C) and liquidus temperatures (705 °C). The temperatures here go confirm with the results described for the (1:1) sample as before for figure 12.

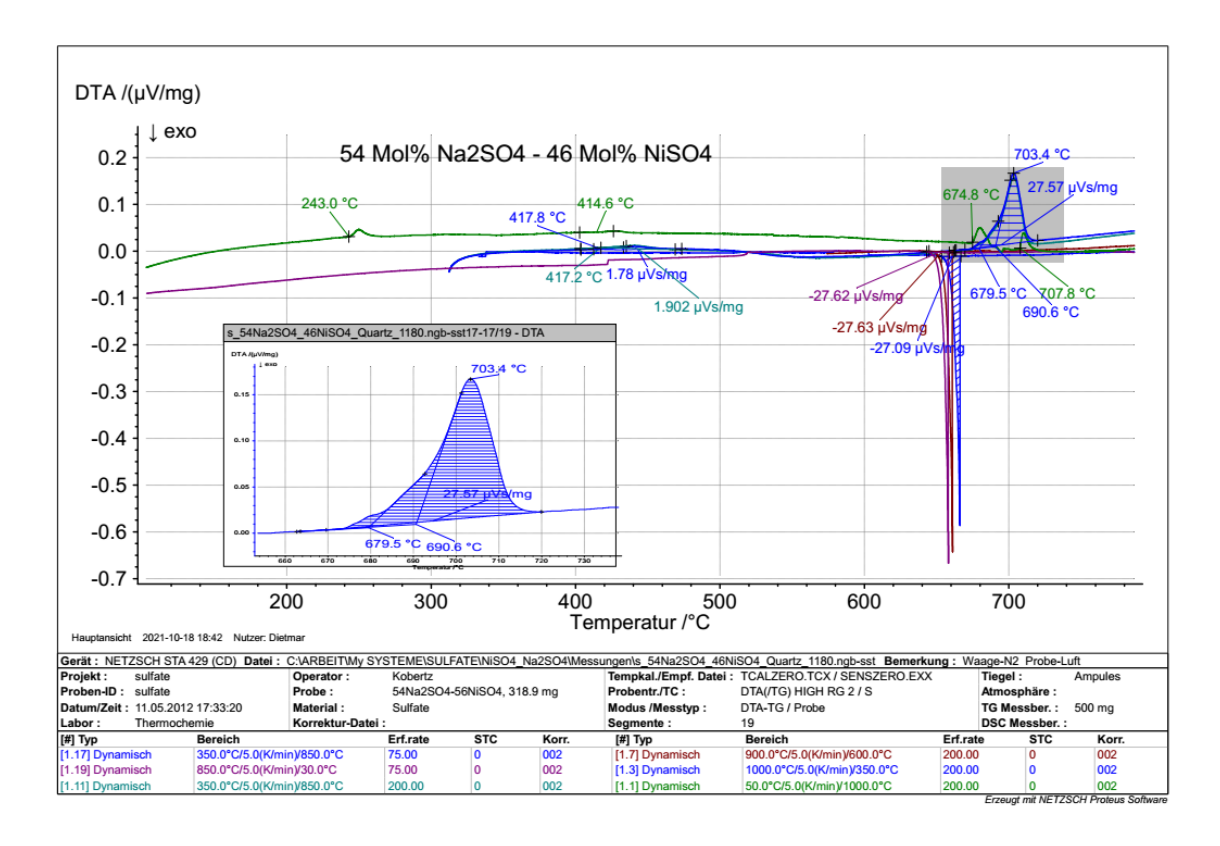


**Figure 13:** The formation of 54 mol%  $Na_2SO_4 - 46$  mol%  $NiSO_4$  is true first time in the second run. Temperatures of decomposition of the 3:1 compound (415 °C), eutectic (680 °C), and liquidus temperatures (703 °C) are seen (raw data).

The thermo analytical measurement on the sample 65 Na<sub>2</sub>SO<sub>4</sub> - 35 NiSO<sub>4</sub> (figure 14) shows the history on the in-situ formation of the equilibrium state. On heating the first time the polymorphism desribed by Kobyashi [23] and Mehrota [24] of Na<sub>2</sub>SO<sub>4</sub> at 210 and 250 °C is still seen (green line), and the signal ends in the liquid phase. On cooling (red line) the liquidus (682 °C) and eutectic transition (674 °C) appear while the Na<sub>2</sub>SO<sub>4</sub> polymorphism disapears. This is the result connected with the formation of the Na<sub>2</sub>SO<sub>4</sub> solid solution. The upper limit decomposition of the Na<sub>6</sub>Ni(SO<sub>4</sub>)<sub>4</sub> is yet not seen before the formation of 3:1 compound. The debut of the decomposition temperature (416 °C) of the 3:1 compound is in the run of the second heating (figure 14).

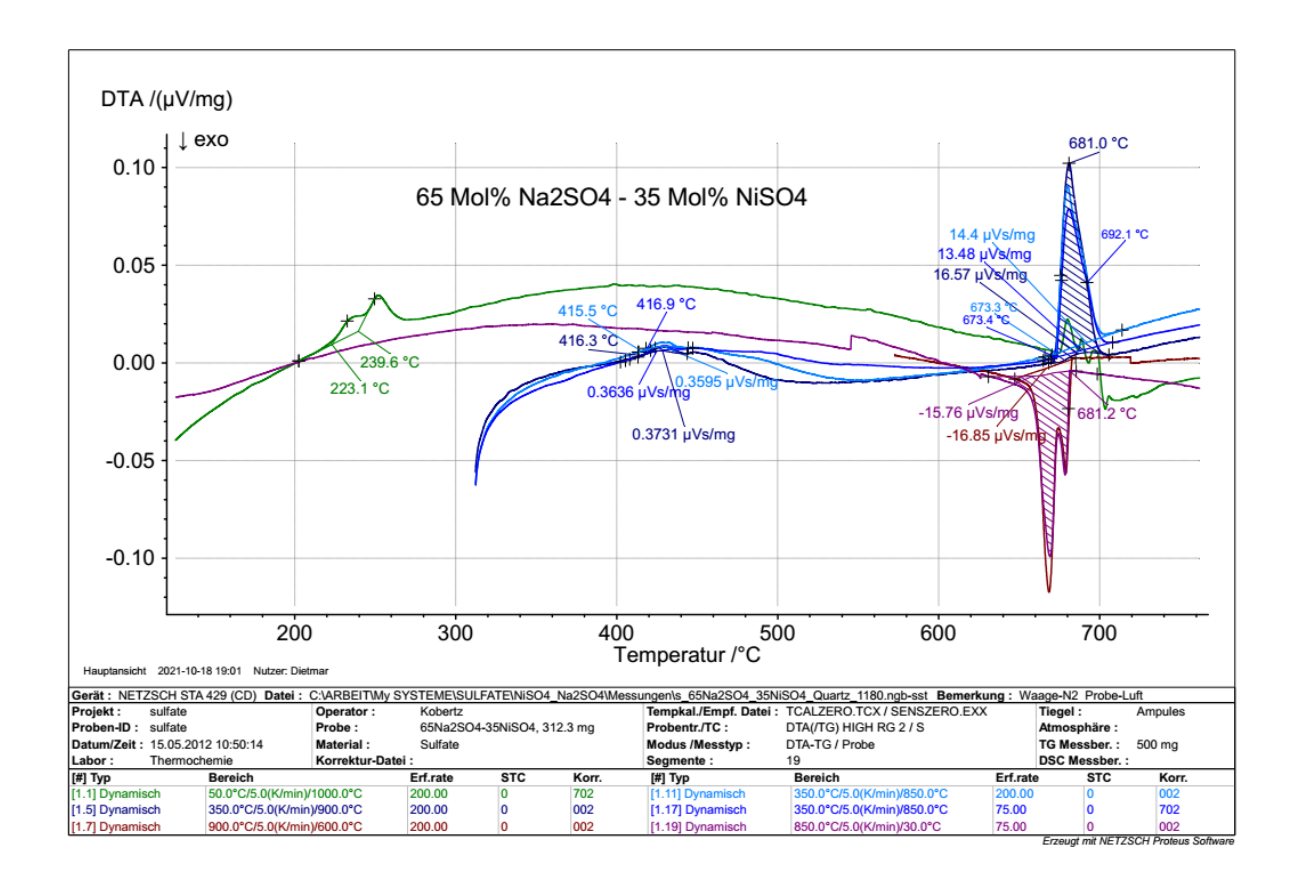


**Figure 14:** DTA respond on 65  $Na_2SO_4 - 35 NiSO_4$ . First run (heating, green and cooling, purple) and second run (heating, blue and cooling, crimson).

DTA measurements on 96 mol%  $Na_2SO_4 - 4$  mol%  $NiSO_4$  show two peaks at 200 °C concerning the two stable modifications of  $Na_2SO_4$ . At high temperature between 865 °C and 882 °C a wide peak represents embedded liquidus and solidus transitions. No further transition was seen between these temperatures. The peak area ( $\mu Vs/mg$ , uncalibrated transition energy) is equal in each case on heating and cooling. All temperatures in the figure 15 are raw data and not yet calibrated.

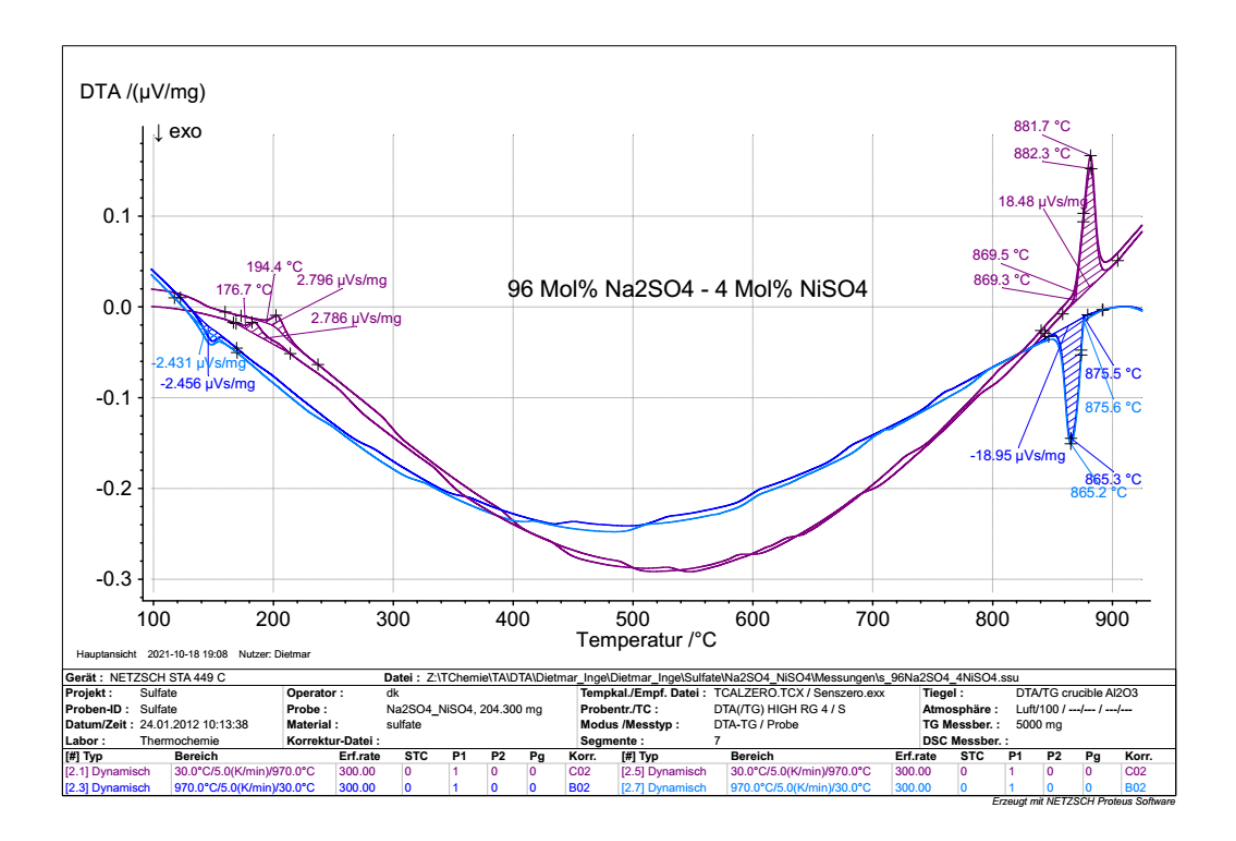


**Figure 15:** DTA response of two runs on  $96 \text{ Na}_2\text{SO}_4 - 4 \text{ NiSO}_4$ . The transition energy given by the peak area is equal on heating red and cooling blue. Between the peaks at 200 and 870 °C no other transition was observed. All temperatures in the figure are raw data and not yet calibrated.

In the end the new phase diagram could be constructed from the thermal analytical transition temperatures and XRD pattern of quenched samples. The system has two compounds, a stable one with an open maximum and one with an upper temperature limit, two eutectics, a structure change at the  $NiSO_4$  - rich part, and a solid solution with different structures at the  $Na_2SO_4$  - rich side (figure 16).

## System Na<sub>2</sub>SO<sub>4</sub> - NiSO<sub>4</sub>

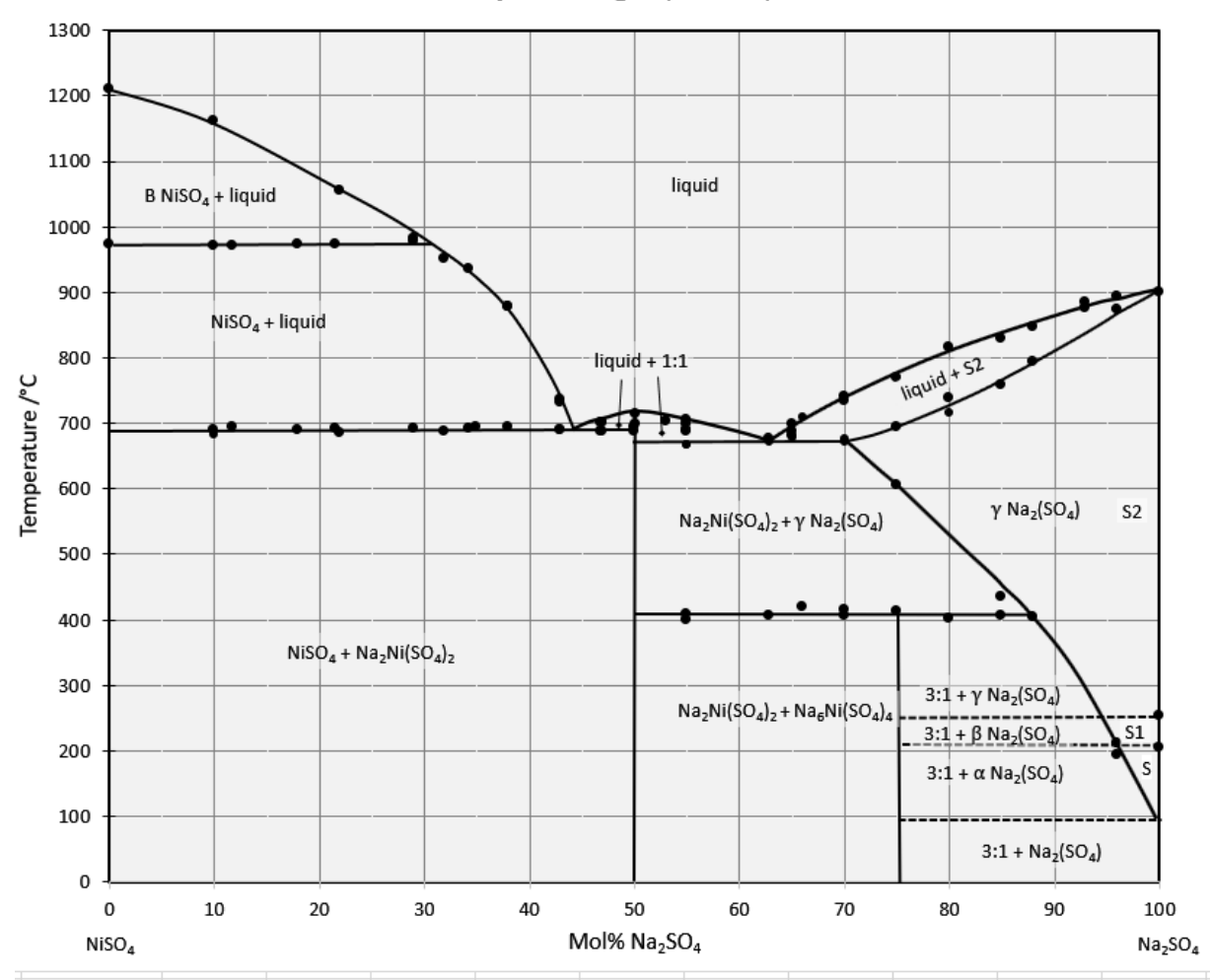


**Figure 16:** Phase diagram of the system NiSO<sub>4</sub> and Na<sub>2</sub>SO<sub>4</sub> based on experimental studies, B NiSO<sub>4</sub> = "dkostruct" [17], 1:1 = Na<sub>2</sub>Ni(SO<sub>4</sub>)<sub>2</sub>, 3:1 = Na<sub>6</sub>Ni(SO<sub>4</sub>)<sub>4</sub>, S =  $\alpha$  Na<sub>2</sub>(SO<sub>4</sub>), S1 =  $\beta$  Na<sub>2</sub>(SO<sub>4</sub>), S2 =  $\gamma$  Na<sub>2</sub>(SO<sub>4</sub>)

Temperatures given in the explaining text parts above are mostly without any calibration but needed to understand the figures of the DTA measurements. The compendium of calibrated numerical values of transition temperatures and ranges in the final phase diagram of the quasi-binary system  $Na_2SO_4$  -  $NiSO_4$  is on display in Table 2.

**Table 2:** Compendium of calibrated transition temperatures and ranges in the phase diagram of the quasi-binary system  $Na_2SO_4$  -  $NiSO_4$ . All temperatures mentioned allover in the text regarding data points in DTA studies are raw data without temperature calibration.

Phase	Temperature ± 3		Range / mol% Na <sub>2</sub> SO <sub>4</sub>	
rnase	K	°C	from	to
Fp NiSO <sub>4</sub>	1483.1	1210.1	0	
"dkostruct" transition	1243.0	970.0	0	
transition range	1243.0	970.0	0	$32 \pm 2$
eutectic temperature 1	962.8	689.8	>0	<50
eutectic mixture 1	962.8	689.8	44 ± 2	
Fp Na <sub>2</sub> Ni(SO <sub>4</sub> ) <sub>2</sub> (1:1)	982.0	709.0	50	
eutectic temperature 2	937.0	664.0	>50	$70 \pm 2$
eutectic mixture 2	937.0	664.0	63±2	
3:1 decomposition	681.7	408.7	>50	87 ± 2
S2 (γ Na <sub>2</sub> SO <sub>4</sub> )	525.1	252.1	$70 \pm 2$	
S1 (β Na <sub>2</sub> SO <sub>4</sub> )	483.5	210.5	94 ± 2	100
S (α Na <sub>2</sub> SO <sub>4</sub> )	371.0	98.0	96 ± 2	
Fp Na <sub>2</sub> SO <sub>4</sub>	1172.3	899.3	100	

# Heat Capacity $(C_p^0)$ of Na<sub>2</sub>Ni(SO<sub>4</sub>)<sub>2</sub>, experimental and calculated

The heat capacity of the 1:1 compound was a crucial factor to perform the studies with caloric methods. Six samples were studied with DSC\_HighT and DSC\_LowT for comparison. The results are shown on figure 17. Both experimental methods give comparable average values of heat capacity with uncertainty around 5%. Studies with DSC are different from DTA since the heating rate is with 15 to 20 K min<sup>-1</sup> closer to adiabatic conditions while the heating rate in DTA is with 5 K min<sup>-1</sup> closer to equilibrium state. Further details regarding this difference are given in Kobertz et al. [19].

Some thermal effect has appeared at temperature of 751 K (478 °C), which could either indicate a structural change of the intermediate compound or a small shift in the composition away from the 1:1 sample. The integration of the peak area gives values around 2.1 kJ/mol.

The existence of the structural change can be excluded due to our DTA results in the NiSO<sub>4</sub>-rich region, where no evidence on the existence of the phase transition in the temperature range between 600 to 800 K was observed.

In the case of a deviation from the 1:1 composition the appeared thermal effect can be related to a phase transition in the  $Na_2SO_4$ -rich region. The two-phase region just after the decomposition process exhibits the 1:1 sample coexisting with  $\gamma$   $Na_2(SO_4)$  that undergoes a solubility limit (see figure 16).

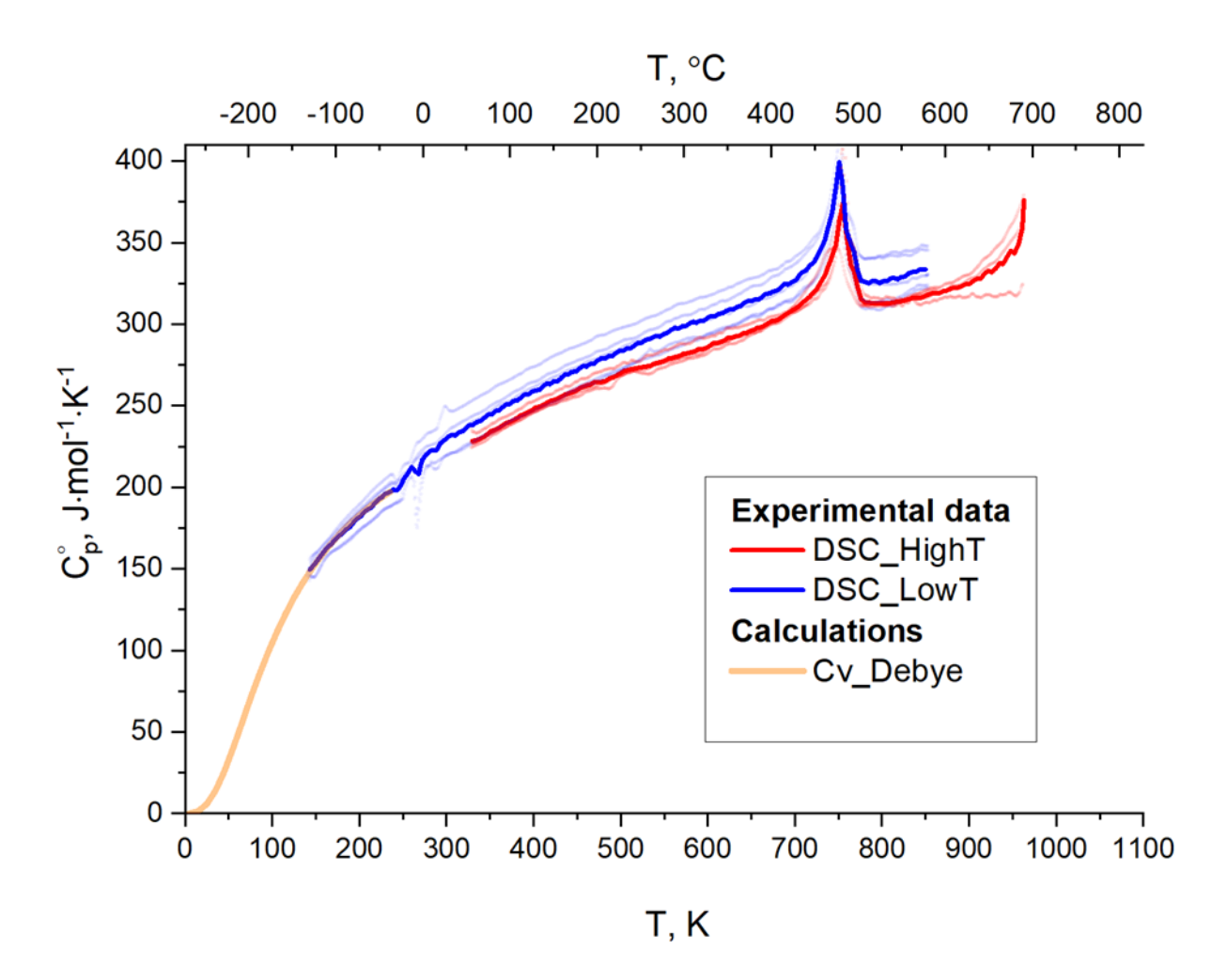


Figure 17. Experimental values of heat capacity measured with DSC\_HighT and DSC\_LowT

To obtain the standard entropy  $S_T^0$  by integrating the Cp(T)/T function, heat capacity below 150 K was calculated using the Debye function [25]:

$$C_V(T) = 9NR \left(\frac{T}{\theta_D}\right)^3 \int_0^{\frac{\theta_D}{T}} \frac{x^4 e^{-x}}{(1 - e^{-x})^2} dx. \tag{4}$$

With  $x = \frac{\theta_D}{T}$ , and  $\theta_D(T)$  = Debye temperature, which was described with the following linear equation (5).

$$\theta_D(T) = 1.8 \, T + 360 \tag{5}$$

in temperature range from 0 K to 300 K. This equation was obtained based on the assumption, that  $C_p \approx C_V$  at low temperatures, (Sergeev et al. [26]). In this case experimental values of heat capacity up to 250 K have been used as a reference for determination of coefficients in the equation (4). The obtained standard entropy is  $S_{298}^{\circ} = 241.6 \text{ J mol}^{-1} \cdot \text{K}^{-1}$ .

The best polynomial describing the experimental DSC data points (blue equation in figure 18) was taken to calculate thermodynamic functions with the *C*p approximation approach of IVTAN [27] and their results are posted in Table 3.

# Heat Capacity of Na<sub>2</sub>Ni(SO<sub>4</sub>)<sub>2</sub>

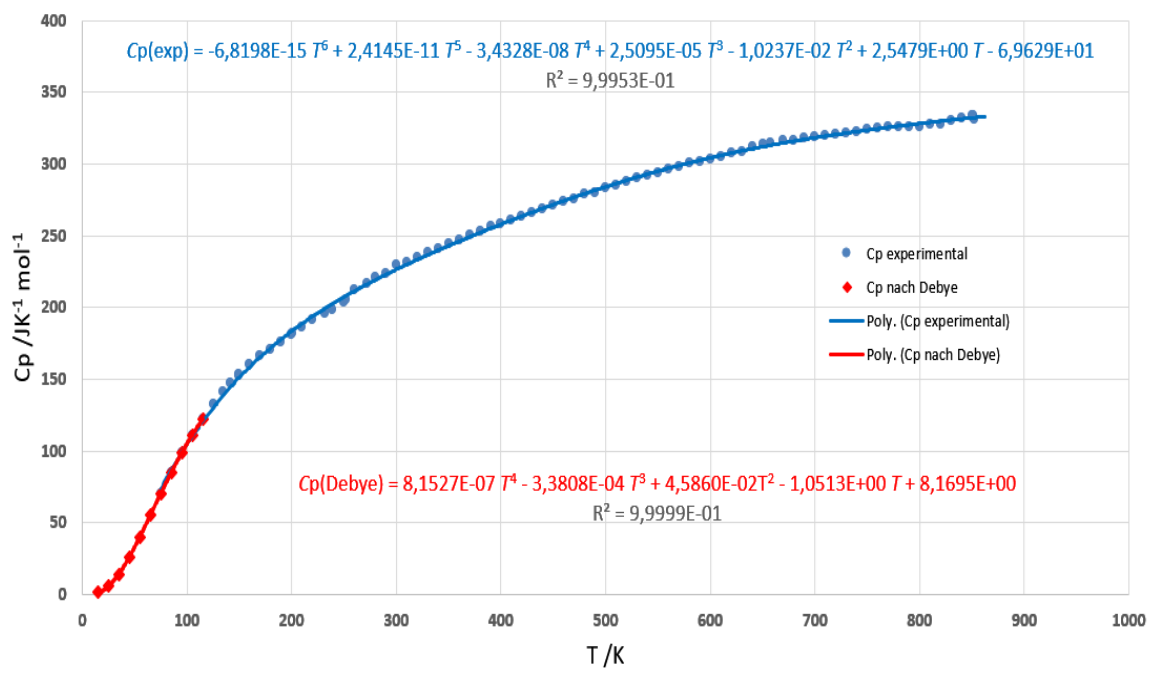


**Figure 18:** Selected  $C_p$  measurements (blue dots) and their polynomial (blue line) of Na<sub>2</sub>Ni(SO<sub>4</sub>)<sub>2</sub>, for T = 40 K to 860 K, IVTAN [27] polynomial approximation in Table 3, Debye [25] approximation (red dots) with polynomial (red line).

**Table 3:** Polynomial coefficients for thermodynamic functions of  $Na_2Ni(SO_4)_2$  (c) from caloric studies for T=40 K to 860 K, Cp approximation with approach of IVTAN [27], x= temperature K/10000. Calculated values using these coefficients are listed in Table 4.

	and instead in Tubic 1.				
$C_{\rm p}^0 = A + \frac{B}{x^2} + C \cdot x + D \cdot x^2 + E \cdot x^3$					
(H <sub>0</sub> – H	$(H^0 - H^0_{298.15})/T = A \cdot x - \frac{B}{x} + \frac{C}{2} \cdot x^2 + \frac{D}{3} \cdot x^3 + \frac{E}{4} \cdot x^4 + F$				
$S^{0} = A \ln(x) - \frac{B}{2 x^{2}} + C \cdot x + \frac{D}{2} \cdot x^{2} + \frac{E}{3} \cdot x^{3} + G$					
$F^{0} = A \ln(x) - \frac{B}{2 x^{2}} + \frac{C}{2} \cdot x + \frac{D}{6} \cdot x^{2} + \frac{E}{12} \cdot x^{3} - F$					
	Temperature range 40 K- 860 K				
A	27.88295				
В	-7.751078 10-4				
С	9.709996 10+3				
D	-1.190341 10+5				
Е	5.576038 10+5				
F	-0.3768432				
G	97.44794				

**Table 4:** Heat capacity  $C_{p\,T}^0$ , and standard values for free energy function ( $F_T^0 = -(G_T^0 - H_{298}^0)/T$ ), the entropy  $S_T^0$ , the enthalpy increment (heat content ( $\Delta H^0 = H_T^0 - H_{298}^0$ )), and Gibbs energy  $G_T^0$  of crystalline Na<sub>2</sub>Ni(SO<sub>4</sub>)<sub>2</sub>(c), T = 40 - 860 K. Equations and parameters are listed in Table 3. Debye standard entropy  $S_{298}^0 = 241.6$  J mol<sup>-1</sup>·K<sup>-1</sup>.

T	$C_{\mathrm{p}T}^{0}$	$F_T^0$	$S_T^0$	$H_T^0 - H_{298}^0$	$G_T^0$
K	J K <sup>-1</sup> mol <sup>-1</sup>			kJ	mol <sup>-1</sup>
298.15	225.48	112.17	241.46	38.548	-33.444
40.00	16.41	4.71	5.62	0.036	-0.188
60.00	60.45	7.38	21.72	0.860	-0.443
80.00	86.12	13.58	42.84	2.341	-1.087
100.00	105.89	21.58	64.25	4.267	-72.158
200.00	176.99	67.90	161.22	18.665	-13.579
300.00	226.25	112.97	242.86	39.966	-72.440
400.00	261.03	154.42	313.01	63.433	-100.317
500.00	285.19	192.38	374.01	90.818	-134.737
600.00	302.19	227.21	427.60	120.232	-174.873
700.00	315.42	259.30	475.20	151.130	-220.057
800.00	328.24	289.01	518.14	183.302	-269.757
860.00	337.13	305.94	542.19	203.256	-301.572

## **Conclusion**

It was the first time to obtain a complete phase diagram of the quasi-binary system  $Na_2SO_4$ -  $NiSO_4$  from room temperature to the liquid phase. It is a two-eutectic system with a miscibility gap on the  $NiSO_4$  rich side, and miscibility gaps and solid solution in the  $Na_2SO_4$  rich part. Two compounds  $Na_2Ni(SO_4)_2$  (1:1) and  $Na_6Ni(SO_4)_4$  (3:1) could be confirmed. The heat capacity  $C_{p(T)}^0$  of the (1:1) compound was determined experimentally from 100 to 860 K and from 0 to 100 K with the Debye approach.  $Na_6Ni(SO_4)_4$  compound exists at lower temperature before it decomposes at  $682 \pm 5$  K. The enthalpy of melting for  $Na_2Ni(SO_4)_2$   $\Delta H_{fus} = 59 \pm 3$  kJ mol<sup>-1</sup>.

The Ni-rich side is stable under pressure of more than four bar partial pressure of the non-condensable gas species  $SO_2$  and  $O_2$  in the system. The melting point of NiSO<sub>4</sub> at  $1483 \pm 3$  K could be confirmed under these conditions. The new structure at  $1243 \pm 3$  K ("dkostruct") of lower density NiSO<sub>4</sub> gives evidence to suggest hot-corrosion processes on turbine blades. Cycling of the volume change in the layer opens induced micropores for the gas species and that keeps the corrosion process running fast.

#### References

- [1] F. Pettit, Hot Corrosion of Metals and Alloys, Oxid Met 76 (2011) 1-21.
- [2] Y. Wang, R. Pillai, E. Yazhenskikh, M. Frommherz, M. Müller, D. Naumenko, Role of Temperature in Na<sub>2</sub>SO<sub>4</sub>–K<sub>2</sub>SO<sub>4</sub> Deposit Induced Type II Hot Corrosion of NiAl Coating on a Commercial Ni-Based Superalloy, Advanced Engineering Materials 22 (2020) 1901244.
- [3] F. Warlimont, Verhalten des Schwefelnickels resp. des Nickelsulfates, Metallurgie 6 (1909) 132-133.
- [4] L. Wöhler, K. Flick, Separation of metal sulphates by selective dissociation., Ber Dtsch Chem Ges 67 (1934) 1679-1683.
- [5] K.A. Bolshakov, P.I. Fedorov, Izuchenie Sistem Sulfat Natriya-Sulfat Kobalta I Sulfat Natriya-Sulfat Nikelya, Zh Obshch Khim+ 26 (1956) 348-350.
- [6] A.G. Ostroff, R.T. Sanderson, Thermal Stability of Some Metal Sulphates, Journal Of Inorganic & Nuclear Chemistry 9 (1959) 45-50.
- [7] L. Cot, Sur le sel double  $Na_2Ni(SO_4)_2$  anhydre et sur ses hydrates, C. R. Seances Acad. Sci.,, ,, 1967, pp. 1955-1957.
- [8] R.A. Rapp, J.H. Devan, D.L. Douglass, P.C. Nordine, F.S. Pettit, D.P. Whittle, HIGH-TEMPERATURE CORROSION IN ENERGY-SYSTEMS, Materials Science and Engineering 50 (1981) 1-17.
- [9] W. Eysel, H.H. Hofer, K.L. Keester, T. Hahn, Crystal-Chemistry and Structure of Na<sub>2</sub>SO<sub>4</sub>(I) and Its Solid-Solutions, Acta Crystallogr. Sect. B-Struct. Commun. 41 (1985) 5-11.
- [10] R.A. Rapp, Hot Corrosion of Materials, High Temperature Science 27 (1989) 355-367.
- [11] M. Wildner, Crystal structure refinements of CoSO<sub>4</sub> and NiSO<sub>4</sub>: very short interpolyhedral O—O contacts, Z. Kristall. 191 (1990) 223-229.
- [12] A.K. Roslik, V.N. Konev, A.M. Maltsev, Some Aspects of the Mechanism of High-Temperature Oxidation of Nickel in SO<sub>2</sub>, Oxid Met 43 (1995) 59-82.
- [13] D. Simon, S.U. Phu, C. Perrin, Atmospheric Corrosion of Nickel Analysis of the Formed Compounds and Mechanisms of the Corrosion, Journal De Chimie Physique Et De Physico-Chimie Biologique 92 (1995) 1179-1194.
- [14] M. Ruzicka, Problems with the preparation of anhydrous single crystal sulphates .1. M<sub>2</sub>+SO<sub>4</sub> (M=Fe, Co, Ni), Cryst. Res. Technol. 32 (1997) 743-747.
- [15] E. Tomaszewicz, M. Kotfica, Mechanism and kinetics of thermal decomposition of nickel(II) sulfate(VI) hexahydrate, Journal of Thermal Analysis and Calorimetry 77 (2004) 25-31.
- [16] R.F.A. Pettersson, F. Karlsson, J. Flyg, Hot corrosion of two nickel-base superalloys under alkali sulfate deposition conditions, Mater High Temp 26 (2009) 251-257.
- [17] M.C.B. Hotz, T.R. Ingraham, Sulphation of Tricobalt Tetroxide and Nickel Monoxide with Fused Soidum Hydrogen Sulphate, Canadian Metallurgical Quarterly 4 (1965) 295-302.
- [18] M.H. Shariat, S.A. Behgozin, A new look at nickel-oxygen-sulfur diagrams, Calphad-Computer Coupling of Phase Diagrams and Thermochemistry 20 (1996) 47-67.
- [19] D. Kobertz, M. Müller, Experimental studies on NiSO<sub>4</sub> by thermal analysis and calorimetry, Calphad: Computer Coupling of Phase Diagrams and Thermochemistry 45 (2014) 55-61.
- [20] Ingraham.Tr, P. Marier, Kinetics of Formation and Decomposition of Nickelous Sulfate, Transactions of the Metallurgical Society of Aime 236 (1966) 1067-1071.
- [21] G. Tammann, Über die Anwendung der thermischen Analyse III, Zeitschrift für anorganische Chemie 47 (1905) 289-313.
- [22] I. FIZ, Inorganic Crystal Structure Database (ICSD), FIZ Karlsruhe GmbH.
- [23] K. Kobayashi, Y. Saito, A MODEL PROPOSED FOR THE INTERPRETATION OF DTA AND X-RAY DATA OF THE III[--]I TRANSITION IN SODIUM-SULFATE, Thermochimica Acta 53 (1982) 299-307.
- [24] B.N. Mehrotra, The Crystal-Structure Of Na<sub>2</sub>SO<sub>4</sub>III, Z. Kristall. 155 (1981) 159-163.
- [25] P. Debye, Zur Theorie der spezifischen Wärmen, Annalen der Physik und Chemie 344 (1912) 789-839.

[26] D. Sergeev, B.H. Reis, M. Ziegner, I. Roslyakova, M. to Baben, K. Hack, M. Müller, Comprehensive analysis of thermodynamic properties of calcium nitrate, The Journal of Chemical Thermodynamics 134 (2019) 187 - 194.

[27] L.V. Gurvich, V.S. Iorish, D.V. Chekhovskoi, V.S. Yungman, IVTANTHERMO - A Thermodynamic Database and Software System for the Personal Computer, NIST Special Database 5, CRC Press and Begell House, Boca Raton, FL,, National Institutes of Standards and Technology: Gathersburg, MD, 1993.